Contrasting impurity scattering and pair-breaking effects by doping Mn and Zn in $Ba_{0.5}K_{0.5}Fe_2As_2$

Peng Cheng,[1] Bing Shen,[1] Jiangping Hu,[1,2] and Hai-Hu Wen[1,*]

[1]*National Laboratory for Superconductivity, Institute of Physics and Beijing National Laboratory for Condensed Matter Physics, Chinese Academy of Sciences, P.O. Box 603, Beijing 100190, China*

[2]*Department of Physics, Purdue University, West Lafayette, Indiana 47907, USA*

(Received 11 January 2010; revised manuscript received 3 May 2010; published 25 May 2010)

Resistivity, Hall effect, magnetoresistance and dc magnetization were measured in Mn- and Zn-doped $Ba_{0.5}K_{0.5}Fe_2As_2$ samples. It is found that the Mn doping can depress the superconducting transition temperature drastically with a rate of $\Delta T_c/\text{Mn-1\%}=-4.2$ K, while that by Zn doping is negligible. Detailed analysis reveals that the Mn doping enhances the residual resistivity (ρ_0) significantly, and induces strong local magnetic moments ($\sim 2.58\mu_B$) which play as pair breakers. While the impurity scattering measured by ρ_0 in the Zn-doped samples is much weaker, accompanied by a negligible pair-breaking effect. A possible explanation is that the impurity scattering by the Zn impurities are mainly small angle scattering (or small momentum transfer), therefore it cannot break the pairing induced by the interpocket scattering and thus affects the superconducting transition temperature weakly.

DOI: 10.1103/PhysRevB.81.174529 PACS number(s): 74.62.Dh, 74.20.Rp, 74.70.Dd, 74.70.Xa

I. INTRODUCTION

The discovery of superconductivity above 50 K in iron pnictides has posed a strong impact in the community of condensed matter physics.[1] One of the key issues here is about the superconducting pairing mechanism. Theoretically it was suggested that the pairing may be established via interpocket scattering of electrons between the hole pockets (around Γ point) and electron pockets (around M point), leading to the pairing manner of an isotropic gap on each pocket but with opposite signs between them (the so-called $S^{\pm}$).[2–5] Meanwhile other models adopt the $S^{\pm}$ pairing gap but assume that the pairing interaction is established via the local magnetic superexchange.[6,7] Besides, by varying the height of the pnictogen to the Fe planes, it was argued that the pairing symmetry may be switched from $S^{\pm}$ to d-wave pairing,[8] as corroborated by the data in LaFePO where a nodal gap was inferred from the penetration depth measurements.[9,10] Similarly, experimental results about the pairing symmetry remain highly controversial leaving the perspectives ranging from S^{++} wave, to $S^{\pm}$ and to d wave.[9,11–20] Further comprehension to this essential topic is highly desired.

In a superconductor, the disorder induced impurity scattering and pair breaking strongly depend on the very details of the pairing gap, therefore it is informative to detect the disorder scattering effect in the superconducting state. According to the Anderson's theorem,[21] in a conventional s-wave superconductor, nonmagnetic impurities will not lead to apparent pair-breaking effect. However, a magnetic impurity, owing to the effect of breaking the time reversal symmetry, can break Cooper pairs easily. In sharp contrast, in a d-wave superconductor, nonmagnetic impurities can significantly alter the pairing interaction and induce a high density of states (DOS) due to the sign change of the gap on a Fermi surface. This was indeed observed in cuprate superconductors where Zn-doping induces T_c suppression as strong as other magnetic disorders, such as Mn and Ni.[22] As for the pairing through exchanging the AF spin fluctuations between different Fermi pockets with the $S^{\pm}$ pairing, it has been pointed out that nonmagnetic impurities could severely suppress T_c and the gap.[23–31] In this paper, we report the doping effect of Mn and Zn to the Fe sites of superconductor $Ba_{0.5}K_{0.5}Fe_2As_2$. We found that the Mn doping (leading to the magnetic impurities) depresses T_c drastically, while the impurity scattering and suppression to T_c by Zn doping (nonmagnetic scattering centers) is negligible. The contrasting impurity scattering effects as revealed by our results need to be reconciled with the theoretical expectations of the picture of interpocket scattering via exchanging AF spin fluctuations.

II. EXPERIMENTAL

The Mn-doped and Zn-doped polycrystalline samples $Ba_{0.5}K_{0.5}(Fe_{1-x}TM_x)_2As_2$ (TM=Mn and Zn) were fabricated by solid state reaction method.[32] Powders K_3As, FeAs, BaAs, ZnAs, and MnAs were prepared previously as precursors. The samples with different doping concentrations were pressed into pellets under the same pressure, wrapped in Ta foils and sintered under exactly the same conditions to eliminate the possible errors in the sample-making process. The x-ray diffraction (XRD) measurement was performed using an MXP18A-HF-type diffractometer with Cu $K\alpha$ radiation. The analysis of x-ray diffraction data was done by using the softwares POWDER-X and FULLPROF, the obtained results are consistent with each other. The compositions of the samples were examined by scanning electron microscopy (SEM, Hitachi S-4200) and the energy dispersive x-ray analysis (EDX, Oxford-6566). The ac susceptibility measurements were carried out through an Oxford cryogenic system Maglab-EXA-12. The resistivity, magnetoresistance, and Hall effect were measured with a Quantum Design instrument physical property measurement system (PPMS), and the dc magnetization by a Quantum Design instrument superconducting quantum interference device (MPMS-7).

III. RESULTS

A. Magnetic and resistive transitions

In Fig. 1(a), we show the temperature dependence of resistivity of the Mn-doped samples $Ba_{0.5}K_{0.5}(Fe_{1-x}Mn_x)_2As_2$.

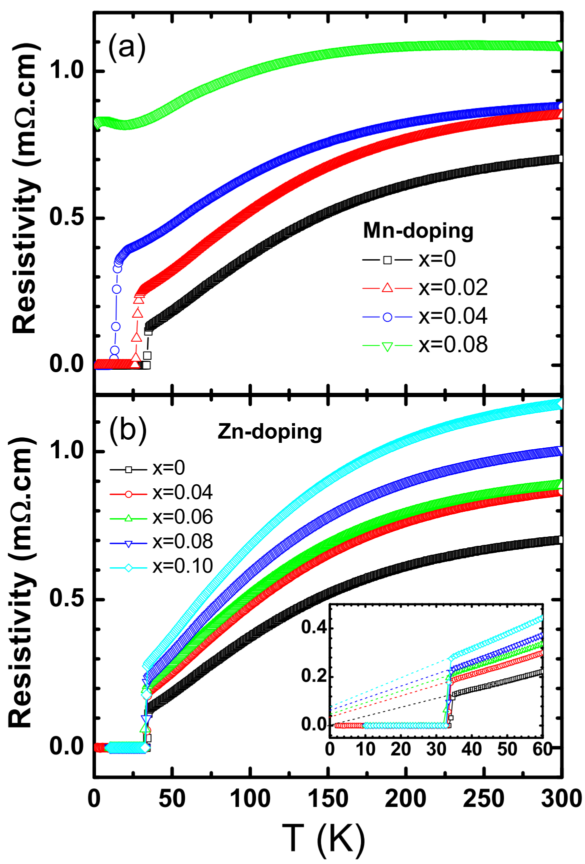

FIG. 1. (Color online) (a) Temperature dependence of resistivity of the $Ba_{0.5}K_{0.5}(Fe_{1-x}Mn_x)_2As_2$ samples under zero field. It is clear that the superconducting transition is depressed drastically by doping Mn. (b) Temperature dependence of resistivity of the $Ba_{0.5}K_{0.5}(Fe_{1-x}Zn_x)_2As_2$ samples under zero field. The depression to the superconducting transition by Zn doping is negligible. The inset in (b) shows the enlarged part in the low temperature region. The dashed lines are extrapolation of the normal state data to $T=0$ K. It is remarkable that the undoped sample has exactly a zero residual resistivity.

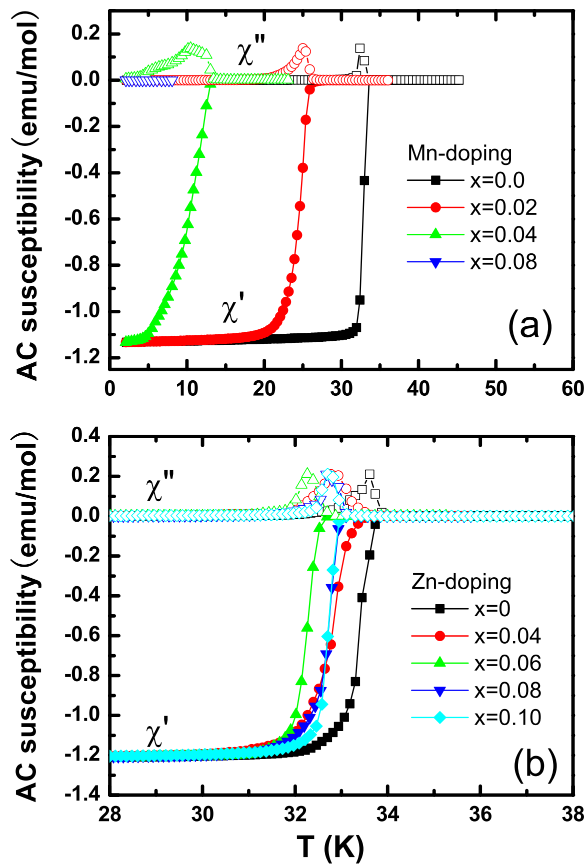

FIG. 2. (Color online) (a) Temperature dependence of ac susceptibility of the $Ba_{0.5}K_{0.5}(Fe_{1-x}Mn_x)_2As_2$ samples measured with $H_{ac}=0.1$ Oe and $f=333$ Hz. (b) Temperature dependence of ac susceptibility of the $Ba_{0.5}K_{0.5}(Fe_{1-x}Zn_x)_2As_2$ samples measured with the same conditions as the Mn-doped sample.

One can see that the superconducting transition temperature was suppressed quickly upon the doping of Mn, and the superconductivity vanishes in the sample with $x=0.08$. In contrast, as shown in Fig. 1(b), the Zn-doped sample does not exhibit a clear change of T_c with the nominal doping concentration as high as $x=0.10$. The Zn-doping effect in the iron pnictide has been under a heavy debate. It was found by Li *et al.*[33] that the Zn doping to the Fe sites in LaFeAsO does not change T_c clearly. However, also in the Zn doped but high pressure synthesized LaFeAsO samples, Guo *et al.*[34] found that the superconductivity can be destroyed completely at a very low doping level of 2%. Actually in our Zn-doped Ba-122 samples, the slight change of T_c in the samples with different Zn concentrations may be attributed to the random scattering of T_c values induced in the synthesizing process. The temperature dependence of ac susceptibilities for the Mn-doped and Zn-doped samples are shown in Figs. 2(a) and 2(b), respectively. For Mn-doped ones, the suppression of T_c is remarkable. The sample with $x=0.08$ does not show diamagnetism down to 2 K. This is consistent with the resistivity data. For Zn-doped ones, however, there are not much differences in the values of T_c for different doping levels ($x=0-0.01$).

B. Structure and composition

In order to know whether the Zn impurities are really introduced into the lattice, we have carried out detailed analysis on the compositions of the grains in each sample using the EDX analysis. The undoped sample $Ba_{0.5}K_{0.5}Fe_2As_2$ exhibits superconductivity at about $T_c=35$ K, combining with the lattice constants,[32] we conclude that our sample is slightly overdoped. The EDX data reveal that the actual doping levels of Mn is very close to the nominal composition up to 8%, while Zn doping has a nonlinear ratio between the really measured composition and the nominal one: $3.1 \pm 0.3\%$ in sample $x=0.04$, about $4.5 \pm 0.5\%$ in the one $x=0.10$. We randomly selected ten typical grains and analyzed the compositions on them. Taking the sample with nominal Zn=10% as an example, the SEM image and EDX analysis process were shown in Fig. 3 and Table I. This fact indicates that the Zn impurities have been successfully doped into the lattice, although the measured composition is lower than the nominal one.

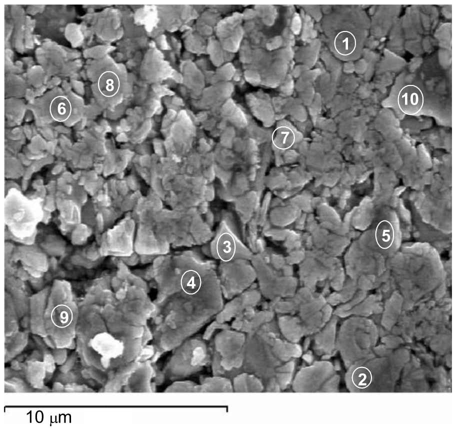

FIG. 3. Scanning electron microscopy image of Zn-doped sample with $x=0.10$. The numbers in the image correspond to the typical grains which we chose randomly to carry out the measurement of energy dispersive x ray. From the EDX data, the compositions of Zn in different grains could be obtained and shown respectively in Table I.

Above discussion can be corroborated by the characterization of the XRD data. The XRD patterns for all samples were shown in Figs. 4(a) and 4(b). For Mn-doped ones, one can see that the phase is rather clean and no impurities could be detected up to $x=0.08$. The lattice constants of a axis and the cell volume increase monotonically with doping of Mn [as shown in Fig. 4(c)], which indicates that the Mn atoms were successfully introduced into the lattice. Assuming that the Mn ionic state is "+2," since the ionic radius of Mn^{2+}(0.8 Å) is bigger than that of Fe^{2+}(0.74 Å), it is understandable that the in-plane lattice constant expands and the unit cell volume increases about 1.6%. While for Zn-doped samples, since the ionic radius for Fe^{2+} and Zn^{2+} are both 0.74 Å, therefore the distortion is much smaller, as evidenced by the slight increase of the unit cell volume (0.34%). In both systems, it is found that the c axis lattice constant does not change obviously compared to the a axis lattice constant.

C. Hall effect, magnetoresistance, and magnetizations

It order to know what has been carried out microscopically through doping Mn and Zn in our samples, we measured the Hall coefficient R_H, Magnetoresistance (MR) and dc magnetization. As shown in Fig. 5(a), R_H is positive in the undoped sample, indicating hole dominant conduction in

TABLE I. The energy dispersive x-ray (EDX) analysis for Zn-doped sample with $x=0.1$.

Grain	Composition	Grain	Composition
1	Zn=4.41%	6	Zn=4.48%
2	Zn=4.23%	7	Zn=3.95%
3	Zn=4.78%	8	Zn=4.53%
4	Zn=5.04%	9	Zn=4.12%
5	Zn=4.58%	10	Zn=4.39%

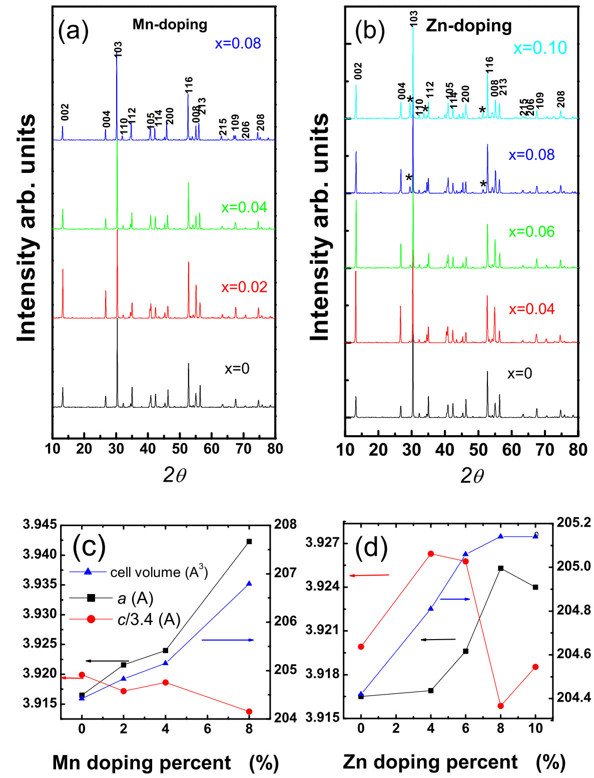

FIG. 4. (Color online) (a) The XRD data for $Ba(Fe_{1-x}Mn_x)_2As_2$ samples. Up to the doping level of 8%, the sample is still quite clean. (b) The XRD data for samples $Ba(Fe_{1-x}Zn_x)_2As_2$ samples. Slight impurity phase emerges when the nominal doping composition goes up to 8%. (c) and (d) show that the doping dependence of the a-axis and c-axis lattice constants, as well as the volume of unit cell. One can see that the a axis changes much larger in percentage compared with the c-axis lattice and the volume expansion is mainly dominated by the a-axis lattice constant.

$Ba_{0.5}K_{0.5}Fe_2As_2$. As we dope Mn into the sample and keep increasing the doped content, the R_H reduces systematically. This can be explained by introducing more holes into the system through Mn doping, though complexity will be brought in understanding the Hall data of the multiband system.[35] Actually doping Mn induces similar effect as doping Cr.[36] The temperature dependence of R_H is also shown for the Zn-doped sample ($x=0.06, 0.08$) in Fig. 5(a). One can see that the data of Zn-doped sample overlap roughly with the undoped one in a broad temperature region, indicating that the Zn^{2+} is almost identical to Fe^{2+} in donating electrons. Figure 5(b) presents the MR of the Mn-doped sample with $x=0.08$, a clear negative MR effect was observed at low temperatures. This negative MR can be easily understood as due to the enhanced electron-spin scattering: doping Mn induces more and more magnetic centers which have stronger magnetic moment compared to that of Fe^{2+}. This argument is supported by the enhanced magnetic susceptibility in the Mn-doped samples. As shown in the inset of Fig. 5(b), the temperature dependence of dc magnetization of the Mn-doped sample can be described nicely by the Curie-Weiss law $\chi=\chi_0+C/(T+T_N)$ with $C=\mu_0\mu_J^2/3k_B$, yielding $\mu_J=0.482\mu_B/(\text{Fe})$ in the undoped sample, $0.645\mu_B/(\text{Fe+Mn})$ in the Mn-doped ($x=0.08$) sample, $0.362\mu_B/(\text{Fe+Zn})$ in the

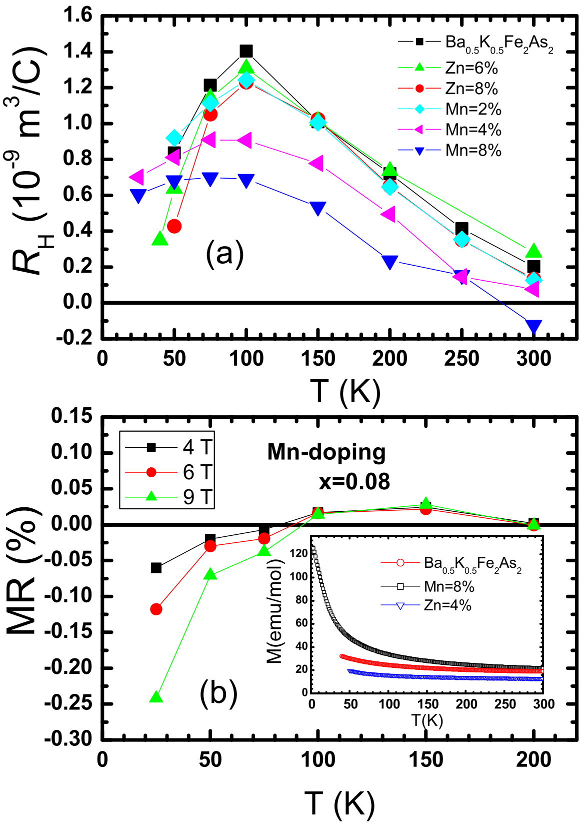

FIG. 5. (Color online) (a) Temperature dependence of Hall coefficient $R_H = \rho_{xy}/H$ measured at 9 T for the undoped, three Mn-doped, and two Zn-doped samples. One can see that by doping more Mn into the system the positive Hall coefficient R_H becomes smaller, indicating the doping of holes into the system. While Zn doping does not change the Hall coefficient too much. (b) MR of the Mn-doped samples, a negative MR was observed here. Inset of (b) shows the temperature dependence of dc magnetization of the undoped, Mn-doped and Zn-doped sample. The $M(t)$ relation can be described by the Curie-Weiss law (see text).

Zn-doped ($x=0.04$) sample. Assuming that each Fe site has also $0.482\mu_B$ in the Mn-doped sample, then each Mn site contributes about $2.58\mu_B$. Zn-doped sample naturally lowers down the paramagnetic susceptibility, suggesting that non-magnetic impurities have been formed. Although it is still under debate whether the AF order is due to the localized moment or itinerant electrons, it is qualitatively correct to make an assessment that the increase of the value of constant "C" in the Curie-Weiss law could be attributed to the enhancement of local magnetic moments upon Mn doping, this argument is also consistent with the negative magnetoresistivity data (Kondo-like scattering).

IV. DISCUSSION

Finally we summarize the main results in Fig. 6. For Mn-doped samples, as the doping concentration increases, T_c decreases quickly with a rate of $\Delta T_c/\text{Mn-}1\% = -4.2$ K, while for the Zn-doped samples the variation in T_c is rather small which could be termed as negligible. According to the Abrikosov-Gorkov formula,[37] if the impurities act as strong

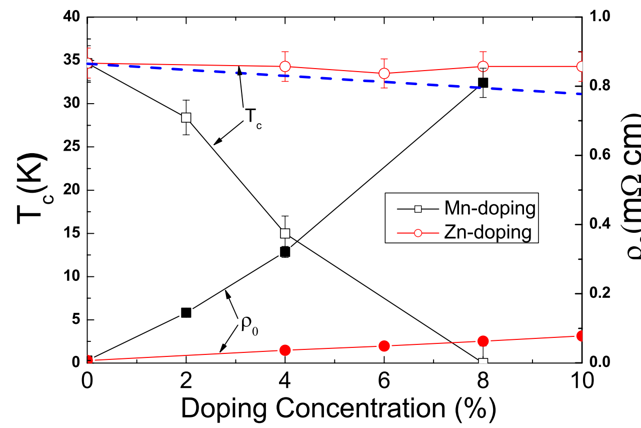

FIG. 6. (Color online) Doping dependence of T_c and ρ_0 in Mn- and Zn-doped samples. The suppression to T_c in Mn-doped samples is drastic, but that by Zn doping is negligible. The enhancement of ρ_0 is much weaker in the Zn-doped sample as compared with the Mn-doped one. The blue dashed line indicates the T_c drop for the Zn-doped samples if we adopt the simple relation $k_B \Delta T_c \propto \rho_0$ and taking the same suppression rate of the Mn-doped system.

pair breakers, the T_c suppression due to pair breaking is essentially related to the impurity scattering rate $k_B \Delta T_c \approx \pi\hbar/8\tau_{imp} \propto \rho_0$, where ρ_0 is the residual resistivity and can be roughly expressed as $m^*/ne^2\tau_{imp}$ in the single band description with n the charge carrier density, m^* the effective mass. Therefore we present also the doping dependence of ρ_0 in Fig. 6. The enhancement of ρ_0 is much stronger for the Mn-doped samples compared with the Zn-doped ones, which indicates different impurity scattering effects in the two sets of samples. For Mn-doped samples, the enhanced average magnetic moments could act as pair breakers and be responsible for the quick suppression of superconducting transition temperature, on the other hand the negative uniaxial chemical pressure effect along the a axis (according to the change of lattice constants) may also have contributions on that. While for Zn-doped samples the residue resistivity does not increases so much, therefore perhaps the impurity scattering by the Zn impurities are mainly small angle scattering (or small momentum transfer), therefore it cannot break the interpocket scattering pairing. This is understandable since the Zn^{2+} and Fe^{2+} have very similar ionic sizes.

One may argue that the weak suppression to T_c in the Zn-doped samples is due to the weak impurity scattering effect (which is actually also very intriguing), however, even taking this small change of ρ_0 in the Zn-doped samples and assuming the same suppression rate $\Delta T_c/\Delta\rho_0$ of the Mn-doped system, we should have a 3.4 K drop of T_c at the doping level of 10%-Zn/Fe. As marked by the blue dashed line in Fig. 6, this is still outer of the range of the data. This result is consistent with the impurity scattering effect by doping other transition metals such as Co and Ni,[38,39] Rh, Ir and Pd to the Fe sites,[40] where no local strong magnetic moments have been detected and the superconductivity are rather robust together with quite strong impurity scattering, as indicated by the large residual resistivity and small residual resistivity ration (RRR) in these materials. The weak impurity scattering as well as the pair-breaking effect given by non-

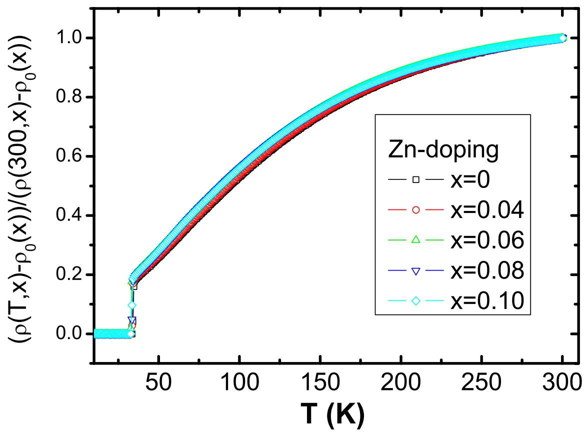

FIG. 7. (Color online) Temperature dependence of $[\rho(T,x)-\rho(0,x)]/[\rho(300\ \mathrm{K},x)-\rho(0,x)]$ for Zn-doped samples with different doping levels, where $\rho(T,x)$ represents the resistivity of the sample at temperature "T" and with doping level "x."

magnetic disorders in iron pnictide may suggest that these dopants all act as impurity scatters with small momentum transfer. By changing the doping level, once this scattering vector in the momentum space is as large as the interpocket vector, we shall see a strong pair-breaking effect, although it is nonmagnetic. It is very worthwhile to check this interesting scenario.

Before concluding the paper, we should mention another interesting discovery in our data. It is found that $[\rho(T,x)-\rho(0,x)]/[\rho(300\ \mathrm{K},x)-\rho(0,x)]$ is doping independent in all temperature regions and all data with different doping levels can be nicely scaled (see Fig. 7). This indicates that, in the single band approach, the $[m^*(x)/\tau(x,T)n(x,T)e^2]/[m^*(0)/\tau(0,T)n(0,T)e^2]$ is temperature independent. Regarding the similar temperature dependence of all the curves, we would assume that $1/\tau(x)\approx 1/\tau(0)$, therefore the temperature independent scaling is due to the electron-boson coupling strength λ in terms of the effective mass relation $M^*(x)=[1+\lambda M^*(0)]$. Suppose that adding Zn has two effects: (1) adding impurity scattering and (2) changing the coupling strength with spin fluctuations (bosons here). The latter assumption is pretty logical in view of the strong effect of Zn on the magnetic properties of the parent compound. If this is true, Zn doping may enhance the superconducting pairing, but unfortunately it is offset by its pair-breaking effect as an impurity. It is very worthwhile to check whether this scaling holds also in other systems.

V. CONCLUDING REMARKS

We fabricated and measured the resistivity, Hall effect, magnetoresistance, and dc magnetization in Mn- and Zn-doped $Ba_{0.5}K_{0.5}Fe_2As_2$ samples. The Mn-doping enhances the residual resistivity and suppresses the superconducting transition temperature drastically. Further analysis indicates that the Mn doping induces strong local magnetic moments ($\sim 2.58\mu_B$) which play as pair breakers. The impurity scattering measured by the residual resistivity ρ_0 in the Zn-doped samples is very weak, accompanied by a negligible suppression to T_c. A possible explanation is that the impurity scattering by the Zn impurities are mainly small angle scattering (or small momentum transfer), therefore it cannot break the pairing given by the interpocket scattering. Finally we found a scaling of the normal state resistivity: $[\rho(T,x)-\rho(0,x)]/[\rho(300\ \mathrm{K},x)-\rho(0,x)]$. This is explained as the enhancement of the coupling strength between electrons and the spin fluctuations induced by the Zn doping.

ACKNOWLEDGMENTS

We appreciate the useful discussions with I. I. Mazin, D.-H. Lee, and G.-M. Zhang. This work is supported by the NSF of China, the Ministry of Science and Technology of China (973 projects: Grants No. 2006CB601000, No. 2006CB921107, and No. 2006CB921802), and the Chinese Academy of Sciences within the Knowledge Innovation program.

*hhwen@aphy.iphy.ac.cn

[1] Y. Kamihara, T. Watanabe, M. Hirano, and H. Hosono, J. Am. Chem. Soc. **130**, 3296 (2008).
[2] I. I. Mazin, D. J. Singh, M. D. Johannes, and M. H. Du, Phys. Rev. Lett. **101**, 057003 (2008).
[3] K. Kuroki, S. Onari, R. Arita, H. Usui, Y. Tanaka, H. Kontani, and H. Aoki, Phys. Rev. Lett. **101**, 087004 (2008).
[4] F. Wang, H. Zhai, Y. Ran, A. Vishwanath, and D. H. Lee, Phys. Rev. Lett. **102**, 047005 (2009).
[5] Z. J. Yao, J. X. Li, and Z. D. Wang, New J. Phys. **11**, 025009 (2009).
[6] K. Seo, B. A. Bernevig, and J. P. Hu, Phys. Rev. Lett. **101**, 206404 (2008).
[7] S. Graser, T. A. Maier, P. J. Hirschfeld, and D. J. Scalapino, New J. Phys. **11**, 025016 (2009).
[8] K. Kuroki, H. Usui, S. Onari, R. Arita, and H. Aoki, Phys. Rev. B **79**, 224511 (2009).
[9] J. D. Fletcher, A. Serafin, L. Malone, J. G. Analytis, J.-H. Chu, A. S. Erickson, I. R. Fisher, and A. Carrington, Phys. Rev. Lett. **102**, 147001 (2009).
[10] C. W. Hicks, T. M. Lippman, M. E. Huber, J. G. Analytis, J. H. Chu, A. S. Erickson, I. R. Fisher, and K. A. Moler, Phys. Rev. Lett. **103**, 127003 (2009).
[11] Y. L. Wang, L. Shan, L. Fang, P. Cheng, C. Ren, and H. H. Wen, Supercond. Sci. Technol. **22**, 015018 (2009).
[12] T. Sato, S. Souma, K. Nakayama, K. Terashima, K. Sugawara, T. Takahashi, Y. Kamihara, M. Hirano, and H. Hosono, J. Phys. Soc. Jpn. **77**, 063708 (2008).
[13] S. Kawasaki, K. Shimada, G. F. Chen, J. L. Luo, N. L. Wang, and G. Q. Zheng, Phys. Rev. B **78**, 220506(R) (2008).
[14] Mu Gang, Zhu Xi-Yu, Fang Lei, Shan Lei, Ren Cong, and Wen Hai-Hu, Chin. Phys. Lett. **25**, 2221 (2008); G. Mu, H. Q. Luo,

Z. S. Wang, L. Shan, C. Ren, and H. H. Wen, Phys. Rev. B **79**, 174501 (2009).
[15] T. Y. Chen, Z. Tesanovic, R. H. Liu, X. H. Chen, and C. L. Chien, Nature (London) **453**, 1224 (2008).
[16] H. Ding, P. Richard, K. Nakayama, T. Sugawara, T. Arakane, Y. Sekiba, A. Takayama, S. Souma, T. Sato, T. Takahashi, Z. Wang, X. Dai, Z. Fang, G. F. Chen, J. L. Luo, and N. L. Wang, EPL **83**, 47001 (2008).
[17] K. Hashimoto, T. Shibauchi, T. Kato, K. Ikada, R. Okazaki, H. Shishido, M. Ishikado, H. Kito, A. Iyo, H. Eisaki, S. Shamoto, and Y. Matsuda, Phys. Rev. Lett. **102**, 017002 (2009).
[18] H.-J. Grafe, D. Paar, G. Lang, N. J. Curro, G. Behr, J. Werner, J. Hamann-Borrero, C. Hess, N. Leps, R. Klingeler, and B. Buchner, Phys. Rev. Lett. **101**, 047003 (2008).
[19] X. G. Luo, M. A. Tanatar, J. P. Reid, H. Shakeripour, N. Doiron-Leyraud, N. Ni, S. L. Budko, P. C. Canfield, H. Q. Luo, Z. S. Wang, H. H. Wen, R. Prozorov, and L. Taillefer, Phys. Rev. B **80**, 140503(R) (2009).
[20] R. T. Gordon, N. Ni, C. Martin, M. A. Tanatar, M. D. Vannette, H. Kim, G. D. Samolyuk, J. Schmalian, S. Nandi, A. Kreyssig, A. I. Goldman, J. Q. Yan, S. L. Budko, P. C. Canfield, and R. Prozorov, Phys. Rev. Lett. **102**, 127004 (2009).
[21] P. W. Anderson, J. Phys. Chem. Solids **11**, 26 (1959).
[22] G. Xiao, M. Z. Cieplak, J. Q. Xiao, and C. L. Chien, Phys. Rev. B **42**, 8752 (1990).
[23] V. Cvetkovic and Z. Tesanovic, EPL **85**, 37002 (2009).
[24] F. Wang, H. Zhai, and D. H. Lee, EPL **85**, 37005 (2009).
[25] Y. Y. Zhang, C. Fang, X. T. Zhou, K. J. Seo, W. F. Tsai, B. A. Bernevig, and J. P. Hu, Phys. Rev. B **80**, 094528 (2009).
[26] J. Li and Y. P. Wang, EPL **88**, 17009 (2009).
[27] G. Preosti, H. Kim, and P. Muzikar, Phys. Rev. B **50**, 1259 (1994).
[28] Y. Bang, H. Y. Choi, and H. Won, Phys. Rev. B **79**, 054529 (2009).
[29] D. Parker, O. V. Dolgov, M. M. Korshunov, A. A. Golubov, and I. I. Mazin, Phys. Rev. B **78**, 134524 (2008).
[30] S. Onari and H. Kontani, Phys. Rev. Lett. **103**, 177001 (2009).
[31] T. Ng and Y. Avishai, Phys. Rev. B **80**, 104504 (2009).
[32] M. Rotter, M. Tegel, and D. Johrendt, Phys. Rev. Lett. **101**, 107006 (2008).
[33] Y. K. Li, X. Lin, Q. Tao, C. Wang, T. Zhou, L. J. Li, Q. B. Wang, M. He, G. H. Cao, and Z. A. Xu, New J. Phys. **11**, 053008 (2009).
[34] Y. Guo, Y. Shi, S. Yu, A. Belik, Y. Matsushita, M. Tanaka, Y. Katsuya, K. Kobayashi, I. Nowik, I. Felner, V. Awana, K. Yamaura, and E. Takayama-Muromachi, arXiv:0911.2975 (unpublished).
[35] L. Fang, H. Luo, P. Cheng, Z. Wang, Y. Jia, G. Mu, B. Shen, I. I. Mazin, L. Shan, C. Ren, and H. H. Wen, Phys. Rev. B **80**, 140508(R) (2009).
[36] A. S. Sefat, D. J. Singh, L. H. VanBebber, Y. Mozharivskyj, M. A. McGuire, R. Y. Jin, B. C. Sales, V. Keppens, and D. Mandrus, Phys. Rev. B **79**, 224524 (2009).
[37] A. A. Abrikosov and L. P. Gor'kov, Sov. Phys. JETP **12**, 1243 (1961).
[38] M. Sato, Y. Kobayashi, S. C. Lee, H. Takahashi, E. Satomi, and Y. Miura, J. Phys. Soc. Jpn. **79**, 014710 (2010).
[39] S. Matsuishi, Y. Inoue, T. Nomura, Y. Kamihara, M. Hirano, and H. Hosono, New J. Phys. **11**, 025012 (2009).
[40] F. Han, X. Zhu, P. Cheng, G. Mu, Y. Jia, L. Fang, Y. Wang, H. Luo, B. Zeng, B. Shen, L. Shan, C. Ren, and H. H. Wen, Phys. Rev. B **80**, 024506 (2009).